V-notch crack initiation by the coupled criterion considering plasticity

Aurélien Doitrand, Dominique Leguillon

V-notch crack initiation by the coupled criterion considering plasticity

Aurélien Doitrand[a,*], Dominique Leguillon[b]

[a] *Univ Lyon, INSA-Lyon, UCBL, CNRS UMR5510, MATEIS, F-69621, France*
[b] *Institut Jean le Rond d'Alembert, Sorbonne Université, CNRS UMR 7190, F-75005, France*

Abstract

An extension of the coupled criterion (CC) of finite fracture mechanics is proposed in order to assess brittle crack initiation considering plasticity. The main change compared to the classical linear elastic approach consists in considering the plastic strain energy variation due to crack initiation. The proposed approach enables assessing quasi-brittle failure at singularities or stress concentrators in materials exhibiting plastic deformation. It is illustrated on V-notch steel specimens subjected to bending. If plastic deformation is disregarded, the CC underestimates the failure force compared to those measured experimentally. Considering plasticity yields a better representation of failure force variation as a function of the V-notch angle.

Keywords: Coupled criterion; crack initiation; plasticity

1. Introduction

Brittle crack initiation can be assessed in the framework of Finite Fracture Mechanics (FFM) [1, 2], which considers finite instead of infinitesimal crack increments and thus overcomes LEFM limitation to assess crack initiation. In this framework, the coupled criterion (CC) consists in the combination of a stress and an energy criterion, which enables the determination of crack initiation loading and length [3]. The CC has successfully been applied to predict crack initiation in various configurations detailed in the review papers [4, 5]. The CC was initially developed under the assumptions of small deformations and linear elasticity material behavior, which make its application through match asymptotic (MA) expansions or full Finite Element (FE) numerically efficient [3, 6, 7].

From a theoretical point of view, no restrictions prevent including nonlinearities in the CC implementation. For instance, crack initiation considering geometrical nonlinearities was imple-

*Corresponding author
Email address: aurelien.doitrand@insa-lyon.fr (Aurélien Doitrand)

mented in [8, 9] using a nonlinear crack opening integral, which improved the fracture load prediction for single-lap joint configuration. Crack initiation in silicone adhesive under large deformation was addressed in [10] by means of coupled strain and energy criteria, which enabled well reproducing the crack arrest after initiation observed experimentally. Crack initiation and propagation in damaged materials was also studied, first by Leguillon and Yosibash [11] who applied the MA approach of the CC considering a small damaged zone ahead of a V-notch. Damage was included in the model by modifying the material Young's modulus, strength and toughness. Li *et al.* [12] combined continuum damage model and discontinuous crack initiation based on the CC. It reverted to decreasing the tensile strength with increasing damage variable and considering damage influence on the energy variation, using element erosion to determine the initiation crack length. Crack initiation at a circular hole in PMMA specimens considering material nonlinear elasticity was studied experimentally [13] and using the CC [13, 14, 15]. It was shown that the fracture stress decreased with increasing hole diameters. Minor differences on the failure stress were obtained using either nonlinear elastic or linear elastic material behavior for stress-driven crack initiation. Larger differences were obtained for configurations driven by both stress and energy conditions, still resulting in small differences in terms of crack initiation force [14].

So far, few works addressed crack initiation considering plasticity. Torabi *et al.* [16] studied crack initiation under moderate or large-scale yielding regimes. Disregarding the actual nonlinear material behavior, an equivalent brittle material having the same fracture energy while increasing its tensile strength was considered, which reverted to a classical linear elastic CC approach in which the material tensile strength is artificially increased. Yosibash *et al.* [17] studied crack initiation at a V-notch in high strength steel alloys by applying the classical linear elastic CC approach, thus disregarding nonlinearities induced by the plastic zone ahead of the V-notch. Using either the material yield strength or ultimate tensile strength as the critical stress parameter, the predicted failure forces were underestimated compared to experimental measurements.

The objective of this work is to provide a CC formulation for crack initiation assessment considering plasticity. The CC formulation is proposed in Section 2. Its numerical implementation is described in Section 4 and a confrontation to experimental results taken from [17] is finally presented Section 5.

2. The coupled criterion considering plasticity

The main idea of the CC is to integrate both stress and energy criteria to evaluate the initiation of cracks in a material. When expanding the application of the CC to account for plasticity, this section outlines how both stress and energy considerations are incorporated.

2.1. Energy criterion

Crack propagation can be analyzed using the crack propagation condition defined in Griffith's criterion [18]:

$$\mathcal{G} \geqslant \mathcal{G}_{\mathrm{c}}, \tag{1}$$

where $\mathcal{G}$ is the Energy Release Rate (ERR) and $\mathcal{G}_{\mathrm{c}}$ the critical ERR. The ERR is defined as $\mathcal{G} = dW_{\mathrm{ext}}/dS - dW_{\mathrm{el}}/dS - dW_{\mathrm{pl}}/dS$ to account for the variation in external force work (W_{ext}), and both elastic (W_{el}) and plastic (W_{pl}) strain energy variations due to the crack advance. At a singular point other than a crack, the ERR tends towards 0 for vanishing crack surfaces. Griffith's criterion is thus unsuitable for evaluating crack initiation.

This result suggests that crack initiation must occur across a finite, not infinitesimal, surface. The energy criterion within the coupled criterion follows the principle of energy conservation before and after the crack nucleation over a finite surface. It yields a balance of the variation of external force work (ΔW_{ext}), kinetic energy (ΔW_{k}), elastic strain energy (ΔW_{el}), plastic strain energy (ΔW_{pl}) and crack surface creation energy ($\mathcal{G}_{\mathrm{c}}S$, where S is surface of the crack Γ):

$$\Delta W_{\mathrm{k}} + \Delta W_{\mathrm{el}} + \Delta W_{\mathrm{pl}} + \mathcal{G}_{\mathrm{c}}S = \Delta W_{\mathrm{ext}}. \tag{2}$$

The kinetic energy before crack initiation is null under quasi-static loading conditions, implying that any change in kinetic energy stemming from crack initiation is positive. The energy equilibrium can thus be expressed in a manner resembling Griffith's criterion, where the ERR is substituted with the Incremental Energy Release Rate (IERR), denoted as $\mathcal{G}_{\mathrm{inc}}$:

$$\mathcal{G}_{\mathrm{inc}} = \frac{\Delta W_{\mathrm{ext}} - \Delta W_{\mathrm{el}} - \Delta W_{\mathrm{pl}}}{S} \geq \mathcal{G}_{\mathrm{c}}. \tag{3}$$

For a specified displacement or loading condition (denoted U), the energy criterion delineates

all the crack configurations, denoted as Γ_{G}, for which the energy criterion is met:

$$\Gamma_{\mathrm{G}}(U) = \{\Gamma \mid \mathcal{G}_{\mathrm{inc}}(S, U)) \geqslant \mathcal{G}_{\mathrm{c}}\}. \tag{4}$$

2.2. Stress criterion

The initial concept of the stress condition of the CC, as initially suggested by Leguillon [3], posits that prior to its formation, the stress level over the crack path must be large enough, which writes:

$$f(\underline{\sigma}(\boldsymbol{x}, U)) \geqslant 0 \ \forall \ \boldsymbol{x} \ \in \ \Gamma, \tag{5}$$

where f represents the material strength surface and $\boldsymbol{x}$ the position vector. The material strength surface is defined as the boundary in the principal stress space, determined by the critical failure stress under a continuously increasing and uniform stress state. For crack initiation in homogeneous isotropic materials with a Rankine-like strength surface, the stress condition reverts to comparing the stress component normal to the crack plane (σ_{nn}) with the material tensile strength (σ_{c}) [3, 6, 19]:

$$\sigma_{\mathrm{nn}}(\boldsymbol{x}, U) \geqslant \sigma_{\mathrm{c}} \ \forall \ \boldsymbol{x} \ \in \ \Gamma. \tag{6}$$

The material tensile strength corresponds to the ultimate tensile strength measured by uniaxial tensile test on plain specimen. Other criteria that involve the material shear strength (τ_{c}) can be used, such as principal stress criterion [20, 21], power ellipse criterion [22, 23, 24, 25, 26] or maximum stress criterion [25, 27]. In the present study, we will limit our analysis to a Rankine strength surface. The two unknowns in the stress criterion are the prescribed displacement or loading and the crack surface. It allows determining, for a given loading, the set of cracks $\Gamma_{\sigma}(U)$ for which the stress criterion is satisfied.

$$\Gamma_{\sigma}(U) = \{\Gamma \mid f(\underline{\sigma}(\boldsymbol{x}, U)) \geqslant 0 \ \forall \ \boldsymbol{x} \ \in \ \Gamma\}. \tag{7}$$

2.3. Coupled criterion

Crack initiation is assessed by combining the stress and the energy condition. It reverts to determining the smallest imposed loading U_{c} for which both stress and energy condition are fulfilled and the corresponding crack initiation configuration Γ_{c} (*i.e.* the crack length, in 2D) :

$$\begin{cases} U_{\mathrm{c}} = \min\{U, \Gamma_\sigma(U) \cap \Gamma_{\mathrm{G}}(U) \neq \emptyset\} \\ \Gamma_c = \Gamma_\sigma(U_{\mathrm{c}}) \cap \Gamma_{\mathrm{G}}(U_{\mathrm{c}}) \end{cases} \tag{8}$$

The main difference compared to the CC implementation in the linear elastic case is that there is a loss of linearity between the stress (resp. the IERR) and the applied loading (resp. the square applied loading). It is thus necessary to compute the stress and the energy conditions for several increasing loading levels in order to determine U_{c}. The practical implementation of the CC considering plasticity is discussed in Section 4.

3. Experimental tests and data

Four-point bending V-notched specimens made of AISI 4340 steel alloy with $\omega = 30$ deg., 60 deg. or 90 deg. V-notch angle and tempered either at 150 °C or 170 °C, were tested under quasi-static loading conditions [17]. The specimen geometry is depicted in Fig. 1. The specimen

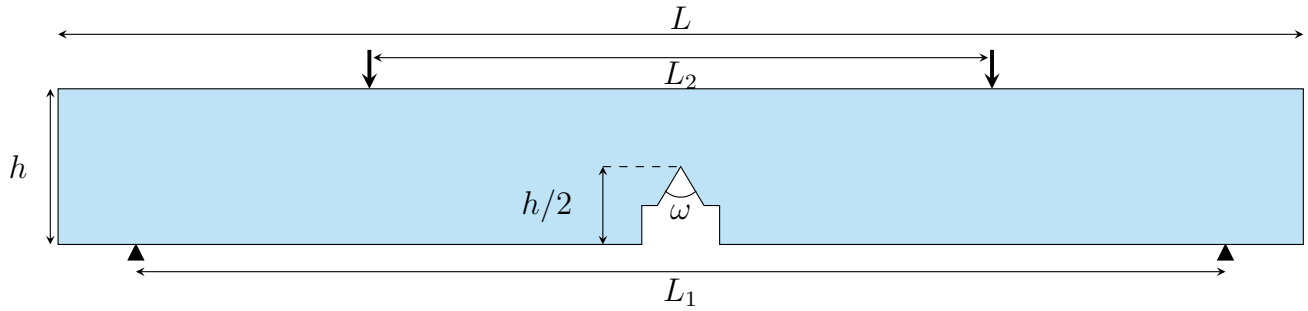

(a)

Figure 1: Four-point bending configuration and specimen dimensions (Length L and width h, support distance L_1, load span distance L_2, V-notch angle ω).

have a 10×10 mm^2 section and are L =80 mm long. The notch depth is half the specimen width. The distance between the lower and upper supports are respectively L_1 =70 mm and L_2 =40 mm (Fig. 1). The rounded V-notch tips exhibit 40 ± 5 µm ($\omega = 30$ deg.), 48 ± 8 µm ($\omega = 60$ deg.), and 71 ± 7 µm ($\omega = 90$ deg.) radii. Brittle fracture of the specimen was observed and the corresponding failure force was measured for the different specimen notch angles and tempering temperatures. The material properties taken from [17] are provided in Table 1, following the experimentally measured stress-strain curves. These experiments were previously analyzed based either with the CC considering a linear elastic material behavior [17], based on a continuum damage model [28] or based on a ductile phase-field fracture description [29]. In the latter work, the comparison to

the experimental measurements was made including a Drucker-Prager criterion with a value of the tensile strength artificially increased to 2.9 GPa so as to recover the failure force measured experimentally on a V-notch specimen.

Tempering temperature	E (GPa)	ν	σ_{y} (GPa)	σ_{c} (GPa)	$\varepsilon_{\mathrm{pl}}^{\mathrm{f}}$	$\mathcal{G}_{\mathrm{c}}$ (kJ/m^2)
150 °C	188	0.3	1.35 $\pm$ 0.02	2.14 $\pm$ 0.01	3.9$\pm$ 0.2 10^{-2}	9.5$\pm$0.7
170 °C	190 $\pm$ 2	0.3	1.48 $\pm$ 0.03	2.07 $\pm$ 0.01	9.2$\pm$ 0.6 10^{-2}	9.7$\pm$1.3

Table 1: Young's modulus (E), Poisson's ratio (ν), yield strength (σ_{y}), tensile strength (σ_{c}), plastic strain at failure ($\varepsilon_{\mathrm{pl}}^{\mathrm{f}}$) and critical energy release rate zzof AISI 4340 steel alloy for 150 °C and 170 °C tempering temperatures.

In the following, the experimental results are used as a comparison with the proposed implementation of the CC considering plasticity.

4. Finite element implementation

In the case of fracture description other than the CC such as, *e.g.*, cohesive zone models [30] or phase-field fracture approach [29, 31], the fracture models already induce nonlinearities even in the case of a linear elastic bulk material behavior. As a consequence, plasticity is accounted for in the energy minimization procedure by considering the plastic energy contribution to the total energy. In the case of the CC, the fracture model itself does not bring any nonlinearities since no process zone is a priori considered. The nonlinearity is only due to the consideration of the material elasto-plastic behavior. The nonlinear CC implementation requires several calculations at different imposed loading magnitudes. For each loading magnitude, stress and energy criteria can be calculated to determine whether the CC is fulfilled or not. The energy change due to plasticity must be considered in the energy balance (See Eq. (3)). In this section, the numerical implementation of the CC is illustrated in the case of a specimen with a 90 deg. V-notch under four-point bending (Fig. 1a) [17]. Due to geometry and loading symmetry, only half of the specimen is modeled using Abaqus (2019) under small deformation and either plane stress or plane strain assumptions. Displacements are prescribed at nodes corresponding to lower and upper support location. The mesh, consisting of four-node linear elements, is refined near the V-notch to ensure that the force at initiation obtained for finer meshes is smaller than 1 %. The minimum mesh size is $10^{-3}h$,where h is the specimen width, which typically results in meshes consisting in about 50000 degrees of freedom. Either linear elastic or elasto-plastic material behavior taken from [17] is considered using Von Mises yielding criterion.

4.1. Energy criterion

For a given imposed displacement, the energy criterion requires the calculation of the i) elastic (Fig. 2a) and ii) plastic (Fig. 2b) strain energy for various crack lengths. The elastic and plastic strain energies are respectively computed as $W_{\text{el}} = \int_V \int_{\underline{\varepsilon}} \underline{\sigma} : d\underline{\varepsilon}^{\text{el}} dV$ and $W_{\text{pl}} = \int_V \int_{\underline{\varepsilon}} \underline{\sigma} : d\underline{\varepsilon}^{\text{pl}} dV$, where $\underline{\varepsilon}^{\text{el}}$ and $\underline{\varepsilon}^{\text{pl}}$ stands for the elastic and plastic strains. For a given crack length, denoted ℓ, this is done by first imposing symmetry conditions all along the specimen middle plane and then releasing the symmetry boundary conditions for all the nodes lying on the crack path. The elastic and plastic strain energy variations between the uncracked and cracked state are then calculated for the corresponding crack length, which also gives the IERR (Fig. 2c). Considering or not plasticity,

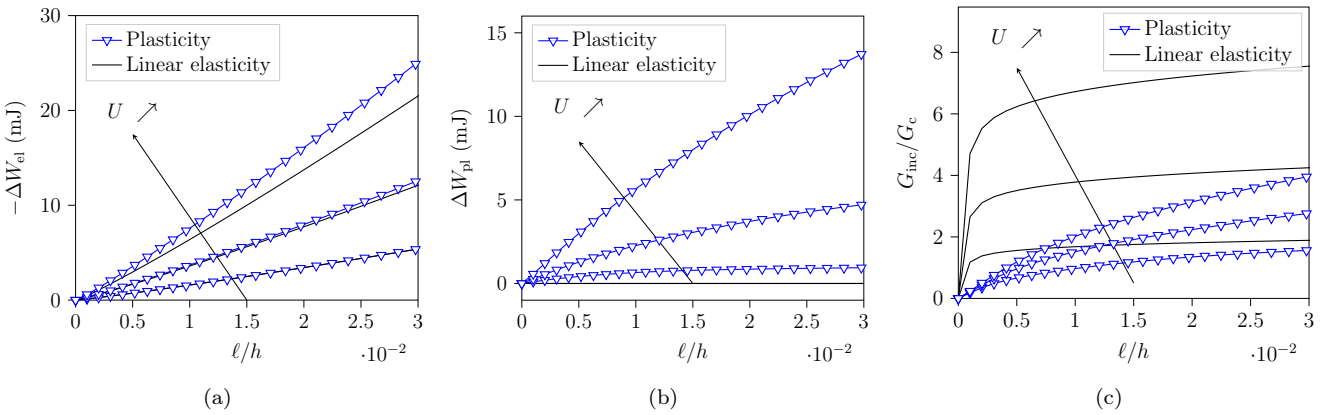

Figure 2: Variation of a) elastic (W_{el}) and b) plastic (W_{pl}) strain energy, and c) normalized IERR ($\mathcal{G}_{\text{inc}}$) as a function of the crack length to specimen width ratio obtained considering plasticity (symbols) or under linear elasticity (plain line) and plane strain assumption. The different curves are obtained for several increasing imposed loading U, as indicated by the arrow.

the elastic strain energy decreases with increasing crack length. For a given crack length, this decrease is larger if plasticity is considered or for larger imposed loadings (Fig. 2a). The plastic strain energy variation increases with increasing crack length and increasing loading (Fig. 2b). For a given crack length, the IERR is smaller if plasticity is considered since a part of the available energy is used to increase the size of the plastic zone due to crack initiation. As a consequence, a larger imposed loading is required to fulfill the energy criterion on a given crack length if plasticity is considered.

4.2. Stress criterion

The normal stress along the anticipated crack path obtained considering or not plasticity is shown in Fig. 3. If plasticity is disregarded, the stress, which is proportional to the imposed loading, is a monotonically decreasing function of the distance to the V-notch tip. Since the stress

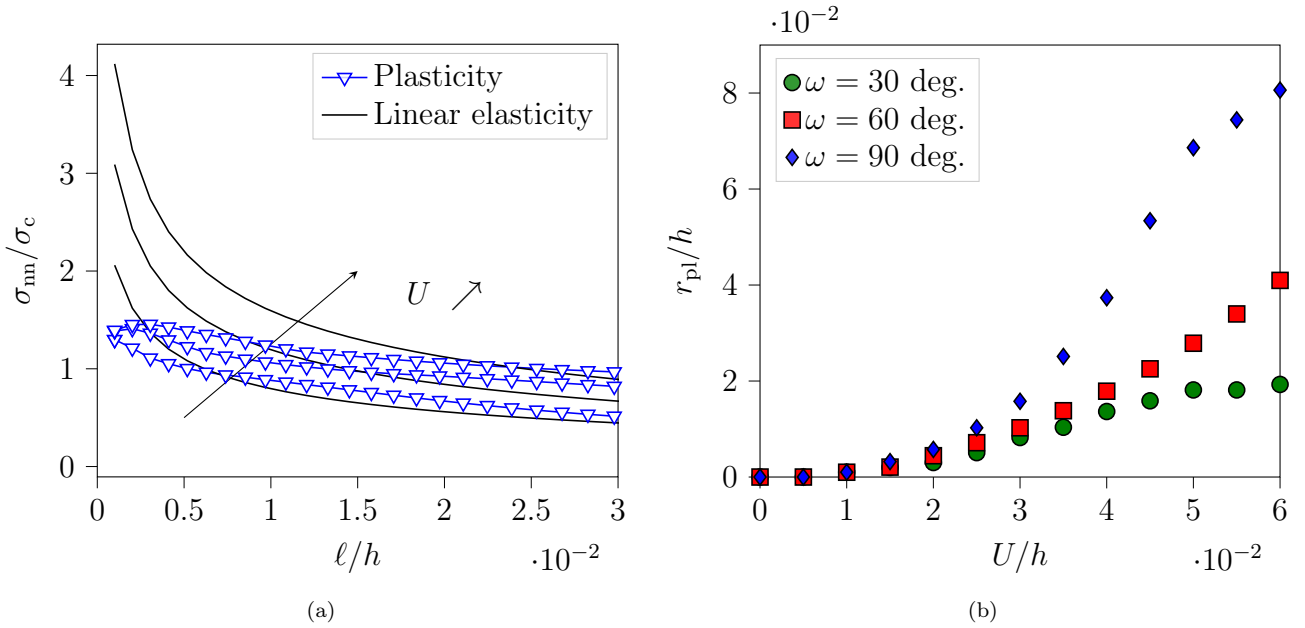

Figure 3: a) Tensile stress (σ_{nn}) to strength (σ_c) ratio as a function of the crack length (ℓ) to specimen width (h) ratio obtained considering plasticity (symbols) or under linear elasticity (plain line) and plane strain assumption for several imposed displacements (U). b) Plastic zone to specimen width ratio as a function of imposed displacement to specimen width ratio obtained for several V-notch angles.

criterion must be fulfilled on the whole crack path before initiation and that the material tensile strength is larger than the material yield strength, it means that the initiation length should be smaller than the plastic zone size r_{pl}. As a consequence, for a given loading, the plastic zone size gives an upper bound for the crack initiation length. Fig. 3b shows the plastic zone size along the specimen middle plane r_{pl} as a function the imposed displacement for the three V-notch angles. It is obtained by performing a first calculation without crack and reporting the distance, along the notch bisector, over which the plasticity criterion is met. In practice, for a given loading level, the energy criterion is only calculated for crack lengths smaller than the plastic zone, which limits the number of total calculations required to apply the CC.

4.3. Coupled criterion

An example of CC solution considering plasticity is given in Fig. 4a that shows the tensile stress to strength ratio and incremental to critical ERR as a function of the crack length to specimen width ratio. As a matter of comparison, the same graph obtained under linear elasticity assumption is shown in 4b. Solving the CC reverts to determining the minimum loading for which both stress and energy criteria are fulfilled. For a too small imposed loading, it is not possible to determine any crack length for which both criteria are fulfilled. Indeed, the minimum length for which the energy criterion is met is larger than the maximum length for which the stress

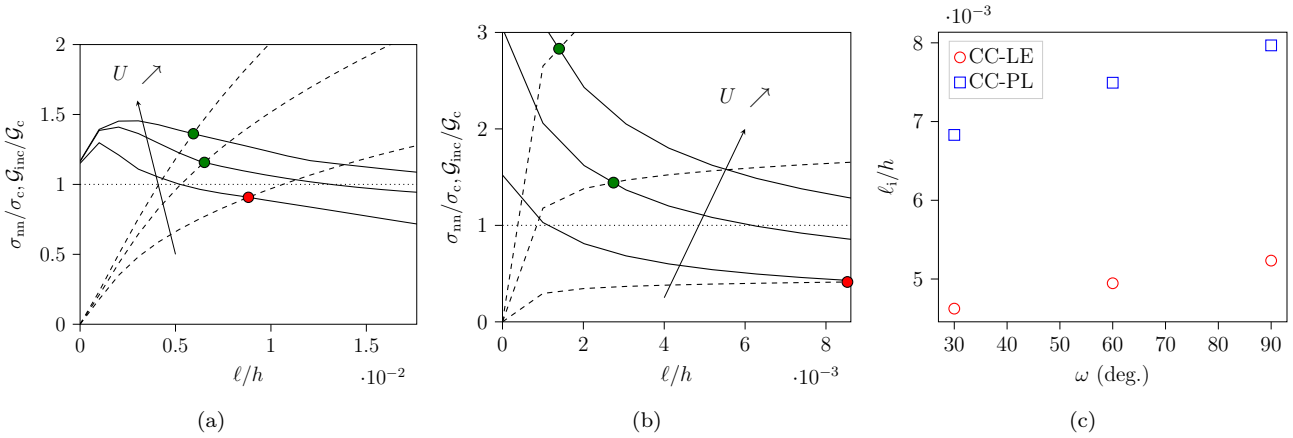

Figure 4: Tensile stress (σ_{nn}) to strength (σ_c) ratio (regular lines) and incremental ($\mathcal{G}_{inc}$) to critical ($\mathcal{G}_c$) ERR (dashed lines) as a function of normalized crack length (ℓ/h) obtained for $\omega = 90$ deg. V-notch angle specimen a) considering plasticity and b) under linear elasticity and plane strain assumption. Green (respectively red) dots represents configurations for which the coupled criterion is fulfilled (respectively not fulfilled). c) Normalized initiation crack length (ℓ_i/h) as a function of the V-notch angle ω obtained considering plasticity(CC-PL) or under linear elasticity assumption (CC-LE).

criterion is met. With increasing loading, the former decreases whereas the latter increases. The loading for which both lengths become equal is the initiation loading. In practice, since several calculations are performed at different loading levels, the initiation loading and crack lengths are finally determined by interpolation of the computed loading levels, similarly to [14]. Fig. 4c shows the initiation length to specimen width ratio as a function of the V-notch angle obtained under linear elasticity or considering plasticity. The initiation length increases in both cases, a larger initiation length being obtained when considering plasticity. This is due to both stress and IERR decrease compared to the linear elastic case (see Fig. 2 and Fig. 3). For a given loading, the length for which the stress criterion is fulfilled decreases whereas the length for which the energy criterion is fulfilled increases. As a consequence, a larger loading level is required in order to fulfill the CC, as well as a larger initiation crack length. The initiation length always remains smaller than the plastic zone extent along the V-notch bisector which is, for 30, 60 and 90 deg. V-notch angle respectively, $r_{pl} = 32 \times 10^{-3}h$, $36 \times 10^{-3}h$ and $47 \times 10^{-3}h$.

5. Comparison with experiments

The proposed implementation of the CC considering plasticity is now compared to experimental tests [17]. The CC is applied to predict the critical force at crack initiation considering plasticity or under linear elasticity and either plane stress or plane strain assumption. A $9.5\,\mathrm{kJ\,m^{-2}}$ (150 °C tempering temperature) or $9.7\,\mathrm{kJ\,m^{-2}}$ (170 °C tempering temperature) critical energy re-

lease rate has been measured based on crack propagation experiments in [17]. The tensile strength corresponds to the ultimate tensile strength measured by uniaxial tensile tests (σ_c =2.14 GPa for 150 °C tempering temperature and σ_c =2.07 GPa for 170 °C tempering temperature). Fig. 5 shows the obtained failure load as a function of the V-notch angle for 150 °C (Fig. 5a) or 170 °C (Fig. 5b) tempering temperatures. If plasticity is disregarded, the failure forces predicted by the CC

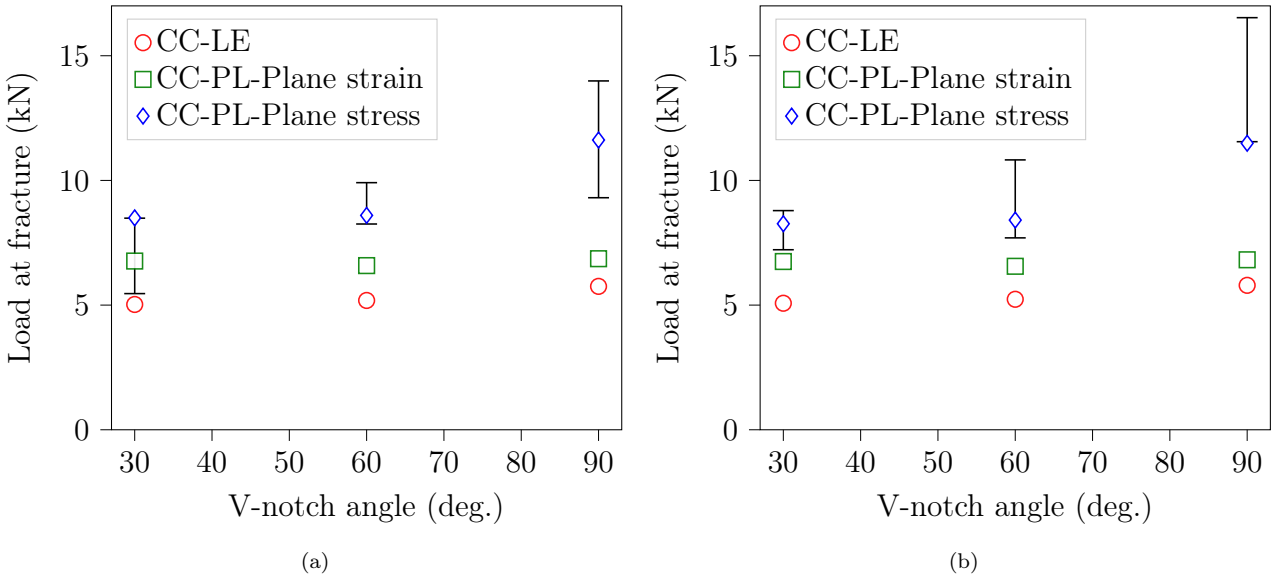

Figure 5: Failure force as a function of the V-notch angle obtained for a) 150 °C or b) 170 °C tempering temperatures obtained for either linear elastic (LE) CC implementation or considering plasticity (PL), using either plane strain or plane stress assumption.

underestimate the failure force measured experimentally whatever the V-notch angles, which is consistent with previous results obtained in [17]. Considering plasticity in the CC implementation results in failure forces that are closer to those measured experimentally. There are two reasons for this behavior, the first one is that a part of the total energy variation is consumed into plastic strain energy increase, the loading must be increased so that enough energy is converted into crack surface creation. The second reason is related to the stress level that is locally smaller than in the linear elastic case, which also tends to increase the imposed loading to fulfill the stress criterion. The failure forces obtained based on plane strain assumption underestimate those obtained based on plane stress assumption. This is due to the the additional contribution of the out-of-plane stress in the plasticity criterion that vanishes for plane-stress assumption, thus resulting in a larger initiation force. The failure forces obtained under plane strain assumption tends to underestimate those obtained experimentally except for 30 deg. V-notch angle. A better description of the failure forces is obtained under plane stress assumption for 60 deg. and 90 deg. V-notch angles.

We finally analyze the influence of the plastic strain energy variation on crack initiation. Eq. (3) can be rewritten as:

$$\frac{\Delta W_{\text{ext}} - \Delta W_{\text{el}}}{S} \geq \mathcal{G}_{\text{c}} + \mathcal{G}_{\text{c}}^{\text{pl}}(S) \tag{9}$$

where $\mathcal{G}_{\text{c}}^{\text{pl}}(S) = \frac{\Delta W_{\text{pl}}}{S}$ corresponds to the ratio between the plastic strain energy variation due to crack initiation and the initiation crack surface. If plasticity is disregarded and that plastic strain energy variation is not included in the energy balance, it thus reverts to applying the CC considering a larger apparent critical ERR $\mathcal{G}_{\text{c}}^{\text{app}} = \mathcal{G}_{\text{c}} + \mathcal{G}_{\text{c}}^{\text{pl}}(S)$ that includes the contribution $\mathcal{G}_{\text{c}}^{\text{pl}}$ coming from plastic strain energy variation due to crack initiation (see Fig. 6). In cases where

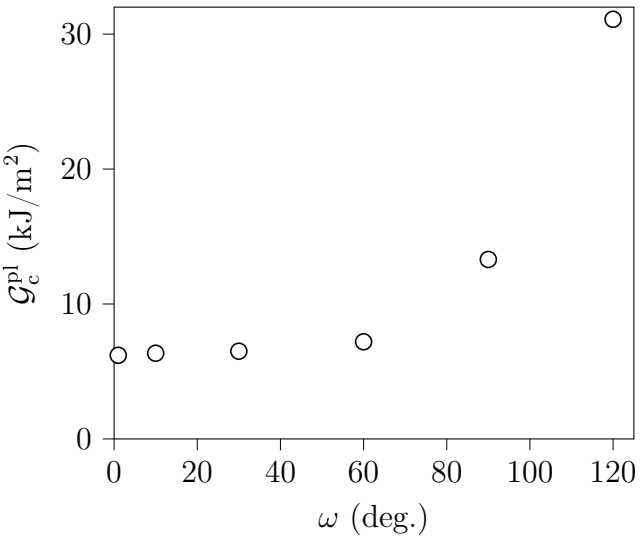

Figure 6: Variation of the apparent critical energy release rate contribution coming from plastic strain energy variation ($\mathcal{G}_{\text{c}}^{\text{pl}}(S)$) as a function of the V-notch angle (ω).

$\mathcal{G}_{\text{c}}^{\text{pl}}(S)$ does not vary much depending on the studied configurations, it thus yields an efficient way to assess crack initiation, phenomenologically considering plasticity through its effect on the critical ERR. Nevertheless, this is not straightforward to consider a constant $\mathcal{G}_{\text{c}}^{\text{pl}}(S)$ as the plastic energy variation contribution increases with increasing initiation crack length and imposed loading. Since the initiation crack length depends on the V-notch angle, it results in increasing $\mathcal{G}_{\text{c}}^{\text{pl}}$ with increasing V-notch angle. Increasing the V-notch angle results in an increase in $\mathcal{G}_{\text{c}}^{\text{pl}}$, from 6.2 kJ m^{-2} to 7.2 kJ m^{-2} for V-notch angles smaller than 60 deg. In this V-notch angle range, the variation of the energy release rate due to the plastic strain energy variation remains smaller than 20 %. For this angle range, the CC could thus be implemented disregarding plasticity and using a larger apparent critical ERR that includes energy dissipation due to both fracture and plasticity. However, this does not hold true for larger V-notch angles for which there is a significant increase in $\mathcal{G}_{\text{c}}^{\text{pl}}$ (Fig.

6). Finally, the ERR contribution coming from plastic strain energy variation depends on the specimen geometry. The classical CC implementation using a larger apparent critical ERR does not seem adapted to predict crack initiation in various specimen geometry for materials yielding. This can be achieved by considering plastic strain energy variation in the energy balance.

6. Conclusion

We extend the coupled criterion of Finite Fracture Mechanics in order to take into account plastic strain energy variation due to crack initiation. The proposed extension remains consistent with the original CC formulation in configurations where no plasticity is involved. Compared to its original form dedicated to study linear elastic configurations, the main change thus relies on considering a nonlinear material behavior as well as the variation of plastic strain energy in the energy balance. Considering plasticity in the CC requires performing several calculations at different imposed loading levels to determine the minimum loading for which both stress and energy conditions are fulfilled. The fulfilment of the stress criterion ensures that the initiation length is smaller than the plastic zone size, which enables limiting the number of possible initiation configurations for a given loading level. Considering plasticity in the CC mainly results in a decrease in the IERR and the stress, and consequently a larger initiation loading level compared to the linear elastic case. Similarly to the case of linear-elastic material behavior, the CC application considering plasticity thus results in a crack jump over a finite length at initiation, which is larger than in the linear-elastic case, yet in the same order of magnitude. Considering plasticity in the CC implementation enables obtaining initiation loadings closer to experimental measurements than assuming linear elasticity for quasi-brittle metals. Future work will cover comparison with other methods such as cohesive zone models [30] or phase-field fracture approach [31, 29], the 3D implementation of the CC considering plasticity, which includes the additional difficulty of determining the 3D initiation crack topology. The evaluation of different node release methods to evaluate the energy criterion, including a progressive node release method, could also be investigated.

7. Acknowledgment

This paper is dedicated to the memory of Dominique Leguillon.
AD would like to thank Zohar Yosibash for insightful discussions about the experiments performed in [17].

References

[1] Z. Hashin, Finite thermoelastic fracture criterion with application to laminate cracking analysis, Journal of the Mechanics and Physics of Solids 44 (7) (1996) 1129–1145. doi:https://doi.org/10.1016/0022-5096(95)00080-1.

[2] J. Nairn, Exact and variational theorems for fracture mechanics of composites with residual stresses, traction-loaded cracks and imperfect interfaces, International Journal of Fracture 105 (2000) 243–271. doi:https://doi.org/10.1016/S1566-1369(00)80012-6.

[3] D. Leguillon, Strength or toughness? a criterion for crack onset at a notch, European Journal of Mechanics - A/Solids 21(1) (2002) 61–72. doi:https://doi.org/10.1016/S0997-7538(01)01184-6.

[4] P. Weißgraeber, D. Leguillon, W. Becker, A review of finite fracture mechanics: crack initiation at singular and non-singular stress raisers, Archive Applied Mechanics 86(1-2) (2016) 375–401. doi:https://doi.org/10.1007/s00419-015-1091-7.

[5] A. Doitrand, T. Duminy, H. Girard, X. Chen, A review of the coupled criterion, hal-04023438 (2024).

[6] A. Doitrand, E. Martin, D. Leguillon, Numerical implementation of the coupled criterion: Matched asymptotic and full finite element approaches, Finite Element in Analysis and Design 168 (2020) 103344. doi:https://doi.org/10.1016/j.finel.2019.103344.

[7] E. Martin, N. Carrère, A fast procedure to predict the notch strength with the coupled criterion, Engineering Fracture Mechanics 284 (2023) 109257. doi:https://doi.org/10.1016/j.engfracmech.2023.109257.

[8] A. Talmon l'Armée, S. Hell, P. Rosendahl, J. Felger, W. Becker, Nonlinear crack opening integral: Mode mixity for finite cracks, Engineering Fracture Mechanics 186 (2017) 283–299. doi:https://doi.org/10.1016/j.engfracmech.2017.10.006.

[9] X. Wei, H. Shen, H. Wang, Fracture failure prediction for composite adhesively bonded double lap joints by an experiment-based approach, International Journal of Adhesion and Adhesives 114 (2022) 103110. doi:https://doi.org/10.1016/j.ijadhadh.2022.103110.

[10] P. Rosendahl, Y. Staudt, A. Schneider, J. Schneider, W. Becker, Nonlinear elastic finite fracture mechanics: modeling mixed-mode crack nucleation in structural glazing silicone sealants, Materials and Design 182 (2019) 108057. doi:https://doi.org/10.1016/j.matdes.2019.108057.

[11] D. Leguillon, Z. Yosibash, Failure initiation at V-notch tips in quasi-brittle materials, International Journal of Solids and Structures 122–123 (2017) 1–13. doi:https://doi.org/10.1016/j.ijsolstr.2017.05.036.

[12] J. Li, D. Leguillon, E. Martin, X. Zhang, Numerical implementation of the coupled criterion for damaged materials, Internation Journal of Solids and Structures 165 (2019) 93–103. doi:https://doi.org/10.1016/j.ijsolstr.2019.01.025.

[13] A. Leite, V. Mantic, F. Paris, Crack onset in stretched open hole pmma plates considering linear and non-linear elastic behaviours, Theoretical and Applied Fracture Mechanics 114 (2021) 102931. doi:https://doi.org/10.1016/j.tafmec.2021.102931.

[14] A. Doitrand, A. Sapora, Nonlinear implementation of Finite Fracture Mechanics: A case study on notched Brazilian disk samples, International Journal of Non-Linear Mechanics 119 (2020) 103245.

[15] X. Chen, A. Doitrand, N. Godin, C. Fusco, Dynamic crack initiation in circular hole pmma plates considering nonlinear elastic material behavior, Theoretical and Applied Fracture Mechanics 124 (2023) 103783. doi:https://doi.org/10.1016/j.tafmec.2023.103783.

[16] A. Torabi, F. Berto, A. Sapora, Finite fracture mechanics assessment in moderate and large scale yielding regimes, Metals 9 (5) (2019) 602. doi:https://doi.org/10.3390/met9050602.

[17] Z. Yosibash, V. Mendelovich, I. Gilad, A. Bussiba, Can the finite fracture mechanics coupled criterion be applied to v-notch tips of a quasi-brittle steel alloy?, Engineering Fracture Mechanics 269 (2022) 108513. doi:https://doi.org/10.1016/j.engfracmech.2022.108513.

[18] A. A. Griffith, The phenomena of rupture and flow in solids, Philosophical Transactions of the Royal Society of London A: Mathematical, Physical and Engineering Sciences 221 (582-593) (1921) 163–198.

[19] P. Rosendahl, P. Weißgraeber, N. Stein, W. Becker, Asymmetric crack onset at open-holes under tensile and in-plane bending loading, International Journal of Solids and Structures 113-114 (2017) 10–23. doi:https://doi.org/10.1016/j.ijsolstr.2016.09.011.

[20] P. Weissgraeber, W. Becker, Finite fracture mechanics model for mixed mode fracture in adhesive joints, International Journal of Solids and Structures 50 (14) (2013) 2383–2394. doi:https://doi.org/10.1016/j.ijsolstr.2013.03.012.

[21] N. Stein, P. Weißgraeber, W. Becker, A model for brittle failure in adhesive lap joints of arbitrary joint configuration, Composite Structures 133 (2015) 707–718. doi:https://doi.org/10.1016/j.compstruct.2015.07.100.

[22] D. Leguillon, S. Murer, A Criterion for Crack Kinking Out of an Interface, Key Engineering Materials 385-387 (2008) 9–12. doi:https://doi.org/10.4028/www.scientific.net/KEM.385-387.9.

[23] M. Muñoz-Reja, L. Távara, V. Mantič, P. Cornetti, Crack onset and propagation at fibre–matrix elastic interfaces under biaxial loading using finite fracture mechanics, Composites Part A: Applied Science and Manufacturing 82 (2016) 267–278. doi:https://doi.org/10.1016/j.compositesa.2015.09.023.

[24] J. Felger, N. Stein, W. Becker, Mixed-mode fracture in open-hole composite plates of finite-width: An asymptotic coupled stress and energy approach, International Journal of Solids and Structures 122-123 (2017) 14–24. doi:https://doi.org/10.1016/j.ijsolstr.2017.05.039.

[25] A. Doitrand, R. Henry, H. Saad, S. Deville, S. Meille, Determination of interface fracture properties by micro- and macro-scale experiments in nacre-like alumina, Journal of the Mechanics and Physics of Solids 145 (2020) 104143. doi:https://doi.org/10.1016/j.jmps.2020.104143.

[26] A. Doitrand, D. Leguillon, G. Molnár, V. Lazarus, Revisiting facet nucleation under mixed mode I+III loading with t-stress and mode-dependent fracture properties, International Journal of Fracture 242 (2023) 85–106. doi:https://doi.org/10.1007/s10704-023-00703-0.

[27] A. Doitrand, D. Leguillon, Comparison between 2D and 3D applications of the coupled criterion to crack initiation prediction in scarf adhesive joints, International Journal of Adhesion and Adhesives 85 (2018) 69–76. doi:https://doi.org/10.1016/j.ijadhadh.2018.05.022.

[28] B. Mittelman, N. Rom, Z. Yosibash, E. Priel, Predicting failure initiation at v-notch tips in an aisi 4340 alloy by a continuum damage model, Engineering Fracture Mechanics 302 (2024) 110067. doi:https://doi.org/10.1016/j.engfracmech.2024.110067.

[29] T. Hu, J. Dolbow, Z. Yosibash, Towards validation of crack nucleation criteria from v-notches in quasi-brittle metallic alloys: Energetics or strength?, Computer Methods in Applied Mechanics and Engineering 402 (2022) 115419, a Special Issue in Honor of the Lifetime Achievements of J. Tinsley Oden. doi:https://doi.org/10.1016/j.cma.2022.115419.

[30] D. S. Dugdale, Yielding of steel sheets containing slits, Journal of the Mechanics and Physics of Solids 8 (2) (1960) 100–104. doi:https://doi.org/10.1016/0022-5096(60)90013-2.

[31] G. Molnár, A. Gravouil, R. Seghir, J. Réthoré, An open-source abaqus implementation of the phase-field method to study the effect of plasticity on the instantaneous fracture toughness in dynamic crack propagation, Computer Methods in Applied Mechanics and Engineering 365 (2020) 113004. doi:https://doi.org/10.1016/j.cma.2020.113004.